Optimization procedure for the cooling of liquid ^{3}He by adiabatic demagnetization of praseodymium nickel

J. M. Parpia, W. P. Kirk, P. S. Kobiela, T. L. Rhodes,[a] Z. Olejniczak, and G. N. Parker

Department of Physics, Texas A&M University, College Station, Texas 77843

(Received 2 July 1984; accepted for publication 21 November 1984)

The construction and performance of a single stage nuclear demagnetization apparatus utilizing 0.267 mole of praseodymium nickel material is described. An optimization procedure to minimize entropy production during the demagnetization of the hyperfine enhanced material has been developed which enabled the cryostat to cool a liquid-^{3}He sample to a temperature of 350 μK. The effects of measured heat leaks and inferred eddy-current heating are accounted for satisfactorily in a model of this procedure.

INTRODUCTION

The study of the superfluid phases of liquid ^{3}He and magnetically ordered phases of solid ^{3}He entails cooling samples to temperatures well below 1 mK. Temperatures below 2.0 mK are unattainable by all but a few high-circulation-rate dilution refrigerators, but can be obtained by the adiabatic demagnetization of copper. However, since the polarization obtained with commercially available superconducting solenoids and dilution refrigerators is modest, the "brute force" nuclear refrigeration technique has involved the construction of relatively massive copper demagnetization stages in order to maintain temperatures below 3 mK for several days.[1] With the discovery by Andres[2] that $PrNi_5$ has a nuclear ordering temperature below 1 mK, and the extensive measurements by the Jülich group[3] of the thermodynamic properties of this hyperfine enhanced material, it was realized that <1 mole of $PrNi_5$ would allow the production of temperatures well below 1 mK for exceedingly long periods.

In this paper we describe the construction, operation, and optimization of a nuclear stage that consisted of ~ 0.27 mole of $PrNi_5$ and ~ 2.8 moles of copper (in the form of a thermal link of wires between the $PrNi_5$ and the main heat exchanger containing a liquid-^{3}He sample). The optimization procedure described in this paper was devised to minimize the production of entropy during demagnetization. From the results of our optimization, inferences can be drawn regarding the magnitude of contributions of various sources of heat leak to the entropy production. Additionally, a lower final temperature of $\lesssim 350\,\mu$K was attained in the liquid sample as compared to 450 μK obtained prior to optimization. In low fields, temperatures below 1.1 mK were maintained for periods exceeding 2 weeks.

I. CONSTRUCTION

A. Cryostat

The cryostat was a S. H. E. model 420 dilution refrigerator insert[4] mounted on a large triangular platform isolated by a loaded air-cushion support system[5] with a ~ 1-Hz resonant frequency. The mechanical isolation was maintained by flexible stainless-steel tubing in the various pumping lines to the refrigerator and a double gimbal arrangement[6] was constructed to decouple the ~ 15-cm-diameter still line.

The exchange gas can was made up of sections of copper tubing, machined to a wall thickness of 0.9 mm and soldered to brass end caps with 95% cadmium, 5% silver solder, which unlike ordinary 40/60 Pb–Sn solder is not superconducting at 4.2 K. Thus, flux jumps due to the demagnetization were avoided. Two radiation shields fixed to the still and to the mixing chamber were fabricated from G-10 glass composite material.[7] The copper cladding supplied on the outside of the shields facilitated thermal contact, but had to be slit in the tail section so as to minimize eddy current heating from the radial field of the magnet during demagnetization.

The demagnetization solenoid[8] was energized by a power supply[9] which was equipped with a voltage comparator and which swept the current at a fixed voltage across the magnet without the use of an analog integrator. At the maximum current rating of 70.8 A, a field of 7.8 T was produced at the magnet's center. The solenoid was compensated to reduce the axial field to <0.05 T at a distance of 24 cm from the center, and this compensation resulted in a maximum radial field of 0.53 T at a distance of 12.5 cm from the magnet's center and 1 cm off axis. The field profile for this magnet is listed in Table I.

B. Nuclear stage and heat exchanger

The nuclear stage consisted of 114 g of $PrNi_5$ compound[10] in the form of eight 6-mm-diameter $\times$ 50-mm-long

TABLE I. The calculated axial field B_z on axis and the radial component B_r for the demagnetization solenoid. The radial component was calculated at a radius of 1 cm.

z (cm)	B_z (T)	B_r (mT)
0	8.00	0
2.5	7.92	30
5.0	7.65	80
7.5	7.07	172
10.0	5.89	341
12.5	3.94	530
15.0	1.89	483
17.5	0.60	265
20.0	0.124	80

 0034-6748/85/030437-07$01.30

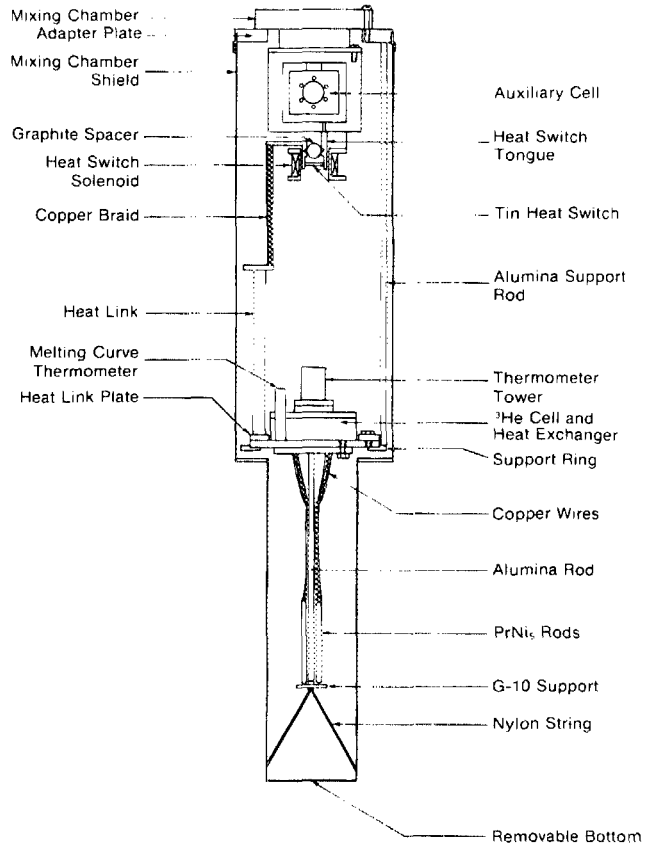

FIG. 1. A schematic view of the nuclear stage illustrating the support structure and construction below the mixing chamber. The still shield, vacuum can, and the magnet are not shown. The heat switch is drawn oversize for clarity.

rods. They were pretinned with 99.99% purity cadmium in a stainless-steel crucible using a solution of zinc chloride as a flux. One hundred copper wires[11] (1 mm diameter × 0.26 m long) were heat treated in a 10-μ air atmosphere at 900 °C for 2 days[12] to produce a residual resistivity ratio (RRR) of 1000. The wires were divided into two bundles, each welded to a large copper plate fabricated from OFHC stock. Each bundle was in turn subdivided into four smaller groups of 12 or 13 wires, with each group arranged around a $PrNi_5$ rod, and then soldered by immersing them individually in the crucible. In order to ensure electrical isolation, the bundles were wrapped with a layer of Teflon tape. The bundles were arranged around a central alumina rod and epoxied to a fiberglass square at the bottom from which fine nylon lines were strung tightly to the mixing chamber shield. Rigidity of the whole assembly was necessary to reduce eddy current losses. Unlike a conventional copper demagnetization stage, the copper wires terminating at a single $PrNi_5$ rod interacted with the radial field of the magnet, which caused eddy currents parallel to the wires. By grouping the bundles of wire close to the axis the effective radial flux could be minimized. The construction details are shown in Fig. 1.

The heat exchanger consisted of a massive copper plate in which slots were milled to leave an array of projecting copper fingers. The interstices were then filled with Druid MD90 powder[13] (copper flakes, 0.2 × 25 × 25 μm) and sintered under pressure. The copper sinter was then drilled with 1-mm-diameter holes at the centers of the squares bounded by the copper posts.[14] A 1-mm gap was left above the sinter region to provide a liquid layer for thermal contact. The heat exchanger had an area of 30 m^2 and contained a 7-ml sample of ^{3}He.

The heat exchanger bottom and the upper plate of the nuclear stage were polished using crocus cloth, etched with dilute nitric acid and then pressed together with eight, 1/4-28 OFHC copper screws tightened to their yield point. The electrical resistance of the press joint was not measured, since previous[17] measurements indicate that the actual thermal resistance exceeds that calculated from the Wiedemann–Franz law. A brass ring fixed to the bottom of the flange was used to support the nuclear stage from the mixing chamber via four alumina rods with brass end caps epoxied at either end. The overall arrangement of the nuclear stage was designed to allow an experimental volume of ~10 cm diameter × 20 cm length above the heat exchanger.

C. Precooling heat link

A 0.95-cm-diameter × 15-cm-long copper heat link rod was welded to a copper ring and had a braid of OFHC copper wires (4655 wires, ~0.05 mm diameter × 8 cm long) welded to its upper end. The heat switch consisted of three, 1.25-mm-diameter × 5.0-mm-long tin wires of 99.9999% purity, arranged perpendicular to the switching field. The heat link was found to have a large thermal resistance probably due to the fine (0.05 mm diameter) copper wires. Nevertheless, the nuclear stage could be precooled to 10.5 mK in 24 h and to its ultimate precool temperature of below 8.0 mK in ~3 days.

D. Thermometry

The thermometry in this apparatus was derived from the susceptibility of lanthanum-diluted cerium magnesium nitrate (LCMN) with a ratio of 19:1 lanthanum:cerium. The 5-mm-diameter × 5-mm-high salt pill and the susceptibility coils were enclosed in a niobium–titanium alloy can to shield against the demagnetization solenoid's fringing field. No special effort was made to screen the earth's magnetic field. The can was immersed in liquid ^{3}He and thermal paths were established by drilling several 1-mm holes through the top of the can. The thermometer was calibrated against a ^{3}He melting curve thermometer (similar to that used by Greywall and Busch[15]) between 50 and 5.5 mK and included as additional calibration points the values of T_A, T_B, and T_S, for the A transition, the B transition, and the solid ordering transition at melting pressure.[16]

E. Thermal resistances

The magnitudes of the thermal impedances between the praseodymium nuclei and the liquid ^{3}He had to be estimated since there were no thermometers to determine the temperature gradient. The thermal resistance of each $PrNi_5$ rod was considered to be in series with that of its copper bundle. The eight rods were in parallel with each other. The effective thermal resistance was in series with that of the press joint and of the heat exchanger.

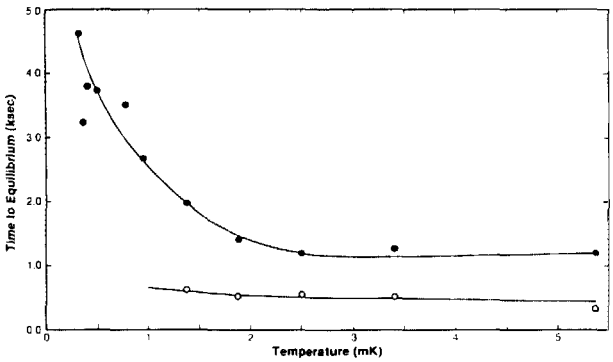

FIG. 2. The thermal relaxation time to equilibrium measured in the melting curve thermometer (○) and in the main heat exchanger (●). The time to equilibrium is the interval elapsed between the completion of a field ramp and equilibrium. The lines drawn through the points are included to guide the eye.

The thermal resistance of the $PrNi_5$ rods may be expressed as $R = A/\kappa r$, where A is the surface area, r the radius of the rod, and $\kappa = 0.15$ T (W/K^{2}m) (similar to steel), and was calculated to be $R = 21/T$ (K^2/W). Each individual wire copper bundle was estimated to have a thermal resistance of $19/T$ (K^2/W). Thus, for eight bundles of resistance $40/T$ (K^2/W) in parallel we calculate the effective resistance to be $5/T$ (K^2/W).

An estimate of the thermal resistance of the press joint was $R = 13/T$ (K^2/W), obtained by scaling the result of Veuro.[17] The thermal resistance of the sinter should be proportional to $1/T$ below 10 mK (Varoquaux[18]). With a measured area of 30 m^2, the thermal resistance of the sintered copper was calculated to be $19/T$ (K^2/W).

F. Thermal relaxation times

We have measured the relaxation times of our two thermometers following a demagnetization to a particular fixed field. The time to equilibrate (Fig. 2) was temperature independent down to ~2 mK for both thermometers and increased below 2 mK only for the LCMN thermometer. This indicated that below 2 mK, the dominant thermal relaxation time of the liquid sample was associated with the heat exchanger itself. This conclusion was confirmed by the large increase in the measured time constants (on the order of 1 day at 0.6 mK and 29 bar) of the LCMN thermometer upon pressurizing the ^{3}He in the main heat exchanger. The mechanism associated with this phenomenon is as yet unknown, but may be associated with the quasiparticle mean free path exceeding a characteristic dimension within the sinter.[18] Nevertheless, at SVP, the time constants are relatively short compared to those measured by other groups.[17,18]

G. Heat leaks

The heat leaks to the nuclear stage fall into three categories. First is the commonly observed time-dependent heat leak. The magnitude of this heat leak was ~35 nW 4 days after the initial transfer of liquid helium, and relaxed roughly exponentially with a decay constant of 1 week to a residual value of 0.7 nW.

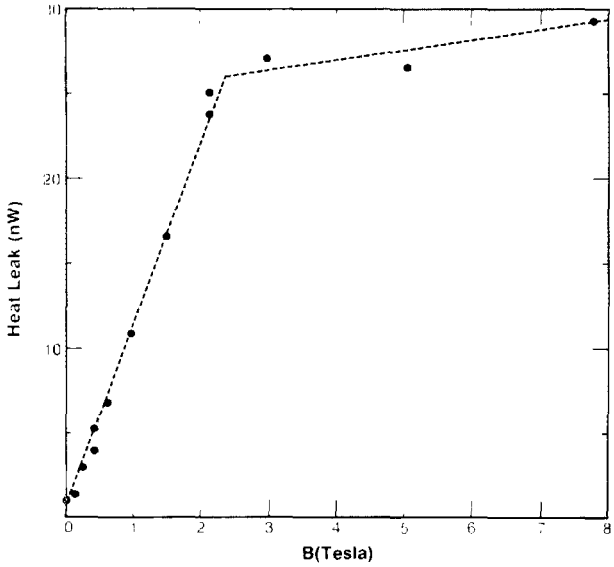

FIG. 3. The measured heat leak in constant magnetic fields between 0 and 7.8 T. The dashed lines are drawn as an aid to the eye.

The last two heat leaks enter into the selection of the optimum demagnetization rate. A field dependent heat leak was measured in the course of a diagnostic demagnetization. The field was reduced in steps, and the heat leak determined from the subsequent measured warm-up rate and the calculated heat capacity (Sec. II A). Figure 3 shows the data for the second type of heat leak. The vibrational nature of this heat leak was verified by noting that on occasions when pressure oscillations occurred in the main helium bath, the heat leak in constant fields increased by 50%. These pressure oscillations were damped by throttling the connection from the main helium bath to our helium recovery system.

The third kind of heat leak was due to eddy currents generated during demagnetizations with an applied field ramp $\dot{B}$. This heat leak can only be generated in four ways, three of which were calculated from known parameters, the fourth being determined from the actual entropy produced during a series of demagnetizations. The contributions from the four parts are (a) currents circulating in the circular cross sections of the wires $[1.7\times10^{-2}\dot{B}^2$ (W s^2/T^2)], (b) currents in the $PrNi_5$ rods $[3\times10^{-4}\dot{B}^2$ (W s^2/T^2)], (c) currents in the cadmium solder $[5.3\times10^{-3}\dot{B}^2$ (W s^2/T^2)], and finally (d) currents along the wires and arising from the removal of the radial field. This last part contributing to the third kind of heat leak, which we identify with a coefficient δ, remains indeterminate due to the complex interconnected geometry of the wires. In summary the eddy current heating can be written as $[2.3\times10^{-2}+\delta]\dot{B}^2$ (W s^2/T^2), where δ had to be determined from the optimized demagnetization rate.

II. OPTIMIZATION

A. Thermodynamics of the nuclear stage

Rather than duplicate the thermodynamic measurements of the Jülich group,[3] we have used their data to compute the entropy and heat capacity of our $PrNi_5$ sample. However, the entropy extracted (ΔS) and the heat capacity of

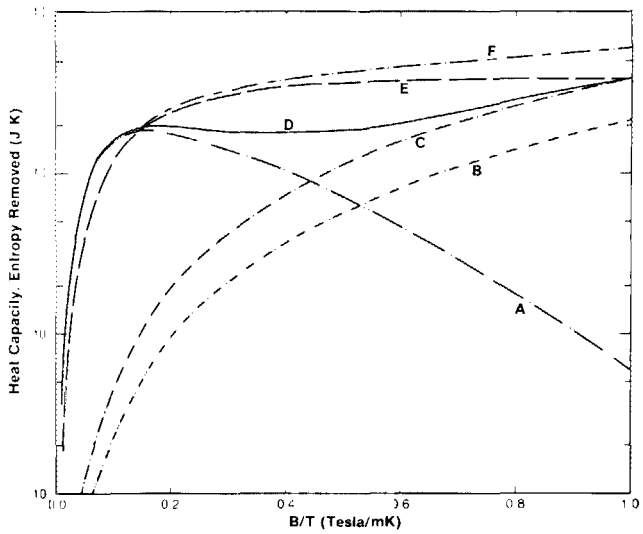

FIG. 4. A plot of the removed entropy and heat capacity of the nuclear stage (0.267 moles of $PrNi_5$, 2.8 moles Cu) against B/T. Note that the curves for the copper reflect the field gradient of the solenoid. (A) The heat capacity of the $PrNi_5$, (B) the removed entropy of the copper, (C) the heat capacity for the copper, (D) the total heat capacity of the nuclear stage, (E) the removed entropy of the $PrNi_5$, (F) the total removed entropy of the nuclear stage.

the copper wires used in the heat link are not negligible and have to be included in the computations of the thermodynamics of the nuclear stage at all but the lowest magnetic field values.

The entropy of a magnetic spin system with spin I is given by the standard[19] relation

$$S/nR = (x/2)\coth(x/2) - (2I+1)(x/2)\coth[(2I+1)x/2] + \ln\{\sinh[(2I+1)x/2]/\sinh(x/2)\},$$

where x is the ratio of the energy difference between the adjacent Zeeman levels to the thermal energy, and is given by the expression

$$x = g_N\mu_N(1+K)B/kT,$$

where g_N is the nuclear g factor, μ_N is the nuclear magneton, and k the Boltzmann constant. It should be noted that $I = 3/2$ for copper and 5/2 for the praseodymium.

Using the values of $g_N = 1.71$ and $(1+K) = 12.2$ for the hyperfine enhancement factor, as quoted in Kubota *et al.*,[3] we find $x/2 = 3.818\,B/T$ for $PrNi_5$, where B is in Tesla and T is in mK.

The specific heat is

$$C/nR = T\,d(S/nR)/dT = (x/2)^2[\operatorname{csch}(x/2)]^2 - (2I+1)^2(x/2)^2 \times\{\operatorname{csch}[(2I+1)x/2]\}^2.$$

At low fields and low temperatures, the effects of ordering of the praseodymium nuclei can be partially accounted for by introducing an internal field $B_{\rm int} \approx 0.066$ T, (Ref. 3). However, the usual expression for the effective field $B_{\rm eff} = (B_{\rm ext}{}^2 + B_{\rm int}{}^2))^{1/2}$, does not fit the data of the Jülich group who found that the internal field enters linearly with the applied field for temperatures below 4 mK and fields below 800 mT.

In Fig. 4, we plot the calculated heat capacity and removed entropy of the $PrNi_5$ (0.267 moles) and of the copper wires (2.8 moles), where the curves for the copper wires reflect the fact that field gradients exist along part of their length (refer to Table I). We have used the full expressions for the thermodynamic quantities rather than the usual quadratic terms in B/T. The resulting total removed entropy and total heat capacity of the nuclear stage are also plotted in the same figure. For B/T greater than 0.2, the heat capacity is constant to within a factor of 2.

B. Optimization procedure

For the purpose of a systematic procedure, it was decided that the demagnetizations would be performed linearly between magnetic field values of 7.8, 5, 3, 2.1, 1.5, and 1.0 T. The rate of demagnetization was varied at these magnetic field values, and the entropy production for a particular lin-

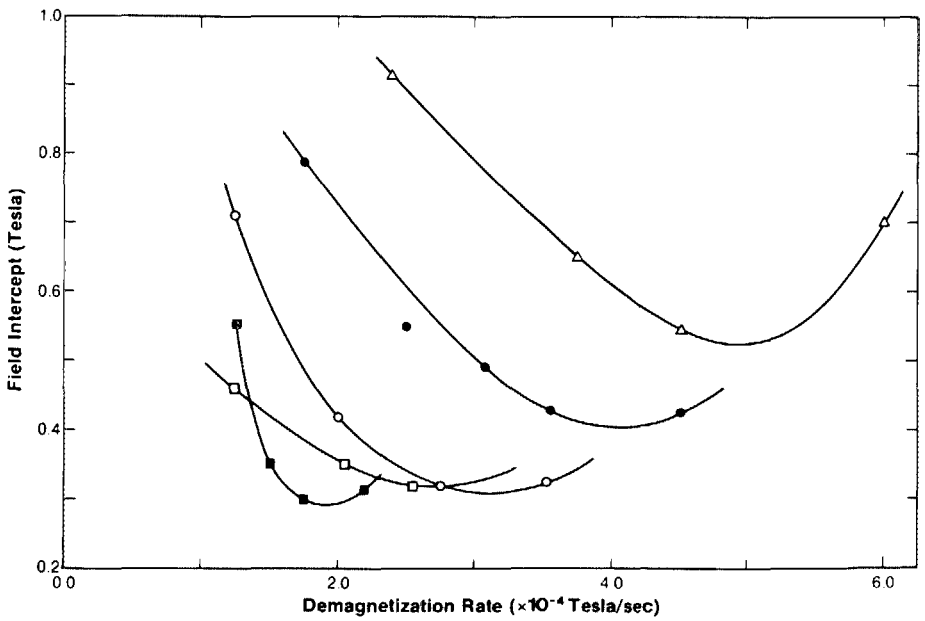

FIG. 5. Plots of the magnitude of the zero temperature magnetic field intercepts obtained by plotting T vs B for several demagnetizations. The intercepts are a measure of the entropy produced from roughly identical starting conditions. The minima in these plots were used to determine the optimum demagnetization. Open triangles are for demagnetizations from 7.8 to 5 T, closed circles for demagnetizations from 5 to 3 T, open circles for demagnetizations from 3 to 2 T, open squares for demagnetizations from 2 to 1.5 T, and closed squares for demagnetizations from 1.5 to 1 T.

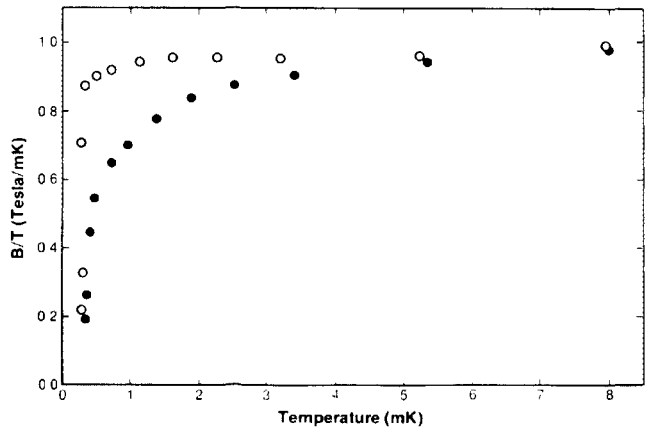

FIG. 6. A plot of the effective magnetic field divided by the temperature vs the temperature (●), where the temperatures are measured in the liquid ^{3}He. By using estimates for the thermal resistance and our determination of the heat leak, the nuclear temperatures T_N are calculated and used to plot [as open points (○)] $B_{\rm eff}/T_N$ vs T_N.

ear demagnetization parametrized. The optimum rate of demagnetization implies a minimum entropy production during a particular field decrement. Since the contributions due to eddy-current heating (δ) could not be calculated, the optimum rate had to be determined operationally. Starting from nearly identical conditions, demagnetizations to the final field values were performed at several rates. By plotting the initial and final coordinate for each decrement on a plot of the temperature versus the applied magnetic field, we were able to parametrize the degree of irreversibility by calculating the "zero temperature" magnetic field intercept B_i (Ref. 20). If the demagnetization were completely reversible, the intercept B_i would be identical to the internal field. A larger intercept would imply that the entropy had increased during the demagnetization. The magnitudes of the resulting intercepts are plotted versus the rate of field removal in Fig. 5 with the curves serving to guide the eye. The procedure was carried out to fields of 0.5 T where the minima became less pronounced and the procedure was then abandoned.

The reversibility of the optimized demagnetization was checked by plotting $B_{\rm eff}/T$ (in Fig. 6) where we have taken the effective field of the $PrNi_5$ to be $B_{\rm eff} = B_{\rm ext} + B_{\rm int}$. If the demagnetization were reversible, the entropy would be constant, and thus B/T would be a constant throughout the demagnetization. The apparent decrease in the quantity B/T did not arise solely from irreversibilities but was partially due to thermal gradients that were set up between the praseodymium nuclei and the thermometers. These thermal gradients primarily resulted from the heat leak shown in Fig. 3. The magnitude of the entropy production was determined by following our demagnetization program to a final field of 1 T and then remagnetizing to 7.8 T. The actual entropy production was $\sim$0.19 J/K during the demagnetization compared to an initial entropy removal of $\sim$5.75 J/K. Knowing the entropy of the nuclei in a 1-T field, the nuclear temperatures could be inferred from the calculated entropy at the end of this diagnostic demagnetization. The thermal resistance was determined from the heat leak and the thermal gradient to be $R \approx 23/T$ (K^2/W), in good agreement with the estimates in Sec. I E. Using this value for the thermal resistance, the nuclear temperature (T_N) was inferred and we also plot $B_{\rm eff}/T_N$ in Fig. 6. The inferred nuclear temperatures will be referred to in Sec. III A.

C. Determination of the eddy current heating

Since the contribution to the entropy production due to eddy currents in the vertical loops of wire in each bundle (δ, Sec. I G) could not be independently calculated, a separate series of diagnostic demagnetizations/remagnetizations were carried out to determine the magnitude of the overall field sweep dependent heating. Demagnetizations between 7.8 and 5 T and subsequent remagnetization to 7.8 T for four different ramp rates were performed, and the overall entropy production for each sequence computed. This total ΔS was then broken up for calculational reasons into two parts $\Delta S_I + \Delta S_{II}$ where the former was the entropy production due to the field dependent heat leak, and the latter was assigned to a rate dependent heat leak. Through our knowledge of the field dependent heat leak $\dot{Q}(B)$, which is shown in Fig. 3, the quantity ΔS_I could be determined by integrating

$$\int_t \frac{\dot{Q}(B)\,dt}{T(t)}$$

for the sequence from 7.8 to 5 T and back up to 7.8 T, where $\dot{Q}(B)$ was assumed to be linear between 7.8 and 5 T. The remaining entropy production contributions ΔS_{II} was therefore determined with fair accuracy from

$$\Delta S_{II} = \int \frac{\dot{Q}(\dot{B})\,dt}{T(t)} = \int \frac{\gamma \dot{B}^2\,dt}{T(t)} = \Delta S - \Delta S_I,$$

where γ is the overall coefficient for eddy current heating caused by the field ramp and was found by this measurement to be $\gamma \approx (0.15 \pm 0.05)\dot{B}^2$(W s^2/T^2). The result for γ was computed from four complete cycles from 7.8 to 5 T and back up to 7.8 T, varying the demagnetization rates by a factor of 4. Consequently, the relative sizes of ΔS_I and ΔS_{II} were varied by over an order of magnitude in order to check the model for consistency. It is clear that the dominant eddy current heating source is δ (due to the radial flux) since the overall coefficient is approximately an order of magnitude greater than from the contributions calculated in Sec. I G.

D. Results of optimization

From the determination of the total entropy production after optimization ($\sim$3.3% to 1 T), it was evident that the overall level of heat leaks to the system was not excessive. The optimization procedure outlined here balanced two "kinds" of heat leaks against one another. The first kind ΔS_I was a heat leak that was observed in a constant field. The origin of this heat leak is thought to be vibrational in nature as it was seen to increase depending on conditions within the main helium bath. A decrease in this heat leak would allow the optimized demagnetization to proceed more slowly.

The more significant heat leak to attempt to decrease is one relating to the coefficient δ due to changes in the magnetic field. It is difficult to ascribe the heating from this source to effects other than the radial magnetic field. A reduction in

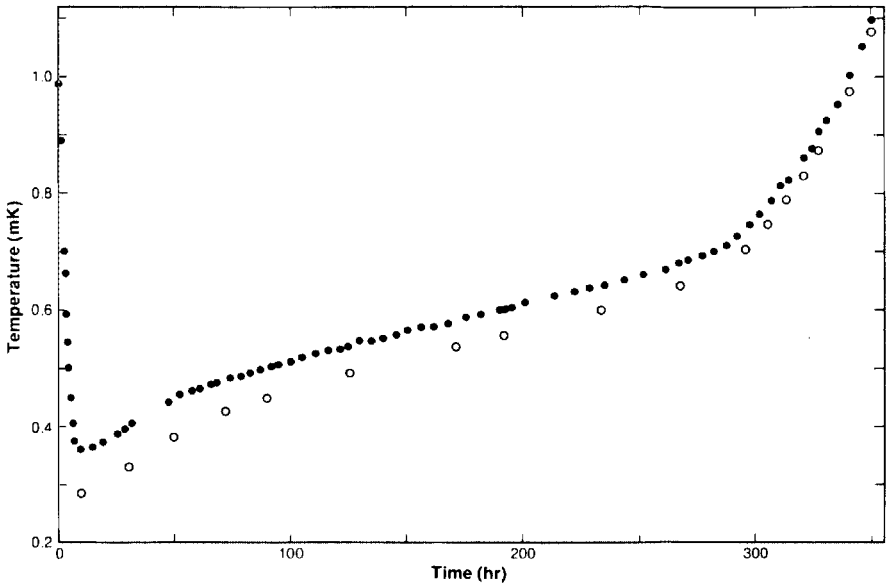

FIG. 7. The time evolution of the ^{3}He temperature after a demagnetization to 0.03 T (●). Also plotted are estimates of the temperature of the praseodymium nuclei under the influence of a 0.7-nW heat leak (○).

δ by an order of magnitude would allow the demagnetization to proceed approximately two to three times faster, an inherent advantage. Such a reduction in the heat leak may be accomplished be reducing the coupling of the radial magnetic field to the nuclear stage, perhaps by employing many small $PrNi_5$ rods, each coupled to the heat exchanger via twisted pairs of copper wires. Alternatively, the wires could be arranged radially so as to minimize flux coupling to the radial field of the solenoid. We would like to emphasize that the coupling to the radial field is not specific to our magnet. The use of compensating coils to reduce the axial magnetic field in the experimental region only results in a large localized radial component to the magnetic field.

III. PERFORMANCE OF THE NUCLEAR REFRIGERATOR

A. Ultimate performance

The lowest temperature achieved in the ^{3}He after optimization was 0.35 mK with a remnant field of 0.03 T. The temperature of the nuclei was estimated to be $\sim$0.28 mK assuming a thermal resistance of $23/T$ (K^2/W) and a 0.7-nW heat leak. The results in Fig. 6 indicate only a small amount of irreversibility above 0.5 mK. Below a 0.5 mK, $B_{\rm eff}/T_N$ apparently decreased sharply, in disagreement with our measurements of the total entropy production, which was estimated as being $\leqslant$25% of total entropy removed for this demagnetization. It is, therefore, likely that the temperatures of the nuclei are considerably lower than those inferred as T_N since, from the observed entropy production, the inferred nuclear temperature should be <0.2 mK rather than 0.28 mK estimated from the thermal resistances and heat leaks. This discrepancy may perhaps indicate that a substantial fraction of the heat leak went directly into the liquid ^{3}He resulting in an additional thermal gradient of $\sim$0.10 mK between the nuclei and the ^{3}He. However, it is more probable that the thermal resistance within the sinter increased rapidly as the quasiparticle mean free path of the ^{3}He exceeds some characteristic dimension in the sinter.[18]

B. Warm-up rate

The feature that distinguishes our $PrNi_5$ nuclear stage from the more conventional copper stages is its ability to maintain temperatures below 1 mK for long periods. The temperature evolution in an ambient field of 0.03 T is plotted in Fig. 7. In practice, by suitably adjusting the residual field (on the order of 0.2 T), temperatures in the range 0.4 to 3 mK can be produced and maintained for several weeks.

IV. DISCUSSION

Our analysis of the performance of the demagnetization stage has given new insight into the performance of $PrNi_5$ material. We have found that liquid-^{3}He temperatures below 0.5 mK are accessible using modest dilution refrigerators and small bore magnets because of the high degree of polarization achieved with hyperfine enhancement systems. We have also seen that, in the design of such a nuclear refrigerator, eddy currents due to the multiply connected nature of the geometry and the radial magnetic field of compensated magnets can restrict optimum demagnetizations to relatively slow ramp rates. However, by modifying the geometry to avoid coupling to the radial component of the field, this restriction could be largely eliminated.

One of our most significant findings is that the ultimate performance, i.e., the lowest temperature achievable, is comparable to that achieved with more massive single stage copper demagnetization cryostats. Consequently, in order to realize the potential performance of this nuclear cooling method, the heat exchanger should be designed for performance at $\sim$0.2 mK with a larger surface area and relatively open geometry. The performance could also be improved by decreasing the thermal resistance in the path between the $PrNi_5$ nuclei and the helium sample by eliminating press contacts. Additionally, the exclusion of materials such as beryllium–copper and indium, which degrade performance because of their quadrupolar heat capacity and/or magnetic impurities below 1 mK, would undoubtedly result in lower realizable temperatures.

Finally, we would like to emphasize that such a hybrid copper and praseodymium–nickel nuclear stage offers significant advantages over larger copper stages, by providing a large, nearly constant, heat capacity at low temperatures.

ACKNOWLEDGMENTS

The systematics of the sintering operation were carried out by R. Borgeson. Helpful conversations with Dr. E. N. Smith and Professor R. C. Richardson are acknowledged. The expert machining skills of J. S. Schwede and R. McBrien have proved to be invaluable. The authors wish to commend L. Richards for production of liquid helium. This research was supported by the National Science Foundation, Division of Materials Research, Low Temperature Physics Program, through Grants No. DMR-8218279 and DMR-8205902. One of us, (JMP) is the recipient of an Alfred P. Sloan Foundation Research Fellowship.

[a] Current address: Department of Physics, University of Texas, Austin, Texas 78712.

[1] K. Andres and O. V. Lounasmaa, *Progress in Low Temperature Physics*, edited by D. F. Brewer (North-Holland, Amsterdam, 1982), Vol. VIII, p. 221.

[2] K. Andres and S. Darack, Physica **86–88B,** 1071 (1977).

[3] M. Kubota, H. R. Folle, Ch. Buchal, R. M. Mueller, and F. Pobell, Phys. Rev. Lett. **45,** 1812 (1980); R. M. Mueller, C. Buchal, H. R. Folle, M. Kubota, and F. Pobell, Cryogenics **20,** 395 (1980).

[4] S. H. E. Corp., 4174 Sorrento Valley Blvd., San Diego, CA 92121.

[5] Newport Corporation, P. O. Box 8020, Fountain Valley, CA 92728.

[6] W. P. Kirk and M. Twerdochlib, Rev. Sci. Instrum. **49,** 765 (1978).

[7] Stevens Products Inc., 128 N. Park St., East Orange, NJ 07019.

[8] American Magnetics Inc., P. O. Box R, Oak Ridge, TN 37830.

[9] Nicolet Nalorac Corp., 1717 Solano Way, Concord, CA 94520.

[10] K. A. Gschneider and B. J. Beaudry, Ames Laboratory, Iowa State University.

[11] Consolidated Wire and Associated Corporations, 1637 S. Clinton St., Chicago, IL 60616.

[12] The procedure used is modified from one derived by S. S. Rosenblum, W. A. Steyert, and F. R. Fickett, Cryogenics **17,** 645 (1977).

[13] Alcan Metal Powders, Box 290, Elizabeth, NJ 07207.

[14] M. Krusius, D. N. Paulson, and J. C. Wheatley, Cryogenics **18,** 649 (1978).

[15] D. S. Greywall and P. A. Busch, J. Low Temp. Phys. **46,** 451 (1982).

[16] W. P. Halperin, F. B. Rasmussen, C. N. Archie, and R. C. Richardson, J. Low Temp. Phys. **31,** 617 (1978).

[17] M. C. Veuro, Acta Polytech. Scand. Appl. Phys. Ser. #**122** (1978).

[18] E. Varoquaux, J. Phys. C **6,** 1603 (1978).

[19] M. W. Zemansky and R. H. Dittman, *Heat and Thermodynamics*, 6th ed. (McGraw Hill, New York, 1979).

[20] H. R. Folle, M. Kubota, Ch. Buchal, R. M. Muller, and F. Pobell, Z. Phys. *B* **41,** 223 (1981).